Proc. Natl. Acad. Sci. USA
Vol. 87, pp. 9052–9056, November 1990
Medical Sciences

Identification and structural analysis of residues in the V1 region of CD4 involved in interaction with human immunodeficiency virus envelope glycoprotein gp120 and class II major histocompatibility complex molecules

(CD4 mutants/protein modeling)

MICHAEL R. BOWMAN*†, KURTIS D. MACFERRIN‡, STUART L. SCHREIBER‡, AND STEVEN J. BURAKOFF*

*Division of Pediatric Oncology, Dana–Farber Cancer Institute, Department of Pediatrics, Harvard Medical School, Boston, MA 02115; and ‡Department of Chemistry, Harvard University, Cambridge, MA 02138

Communicated by Christopher T. Walsh, June 11, 1990 (received for review March 8, 1990)

ABSTRACT **The human CD4 molecule binds both human immunodeficiency virus envelope protein gp120 and class II major histocompatibility complex (MHC) molecules. We have studied a series of mutants in the region of amino acids 42–49 of CD4 for their ability to bind gp120, to interact with class II MHC, to enhance T-cell activation, and to bind a panel of anti-CD4 antibodies. The mutation Q40P (Gln^{40} → Pro) and the deletion d42–49 were found to disrupt most antibody epitopes in the V1 domain of CD4, suggesting major conformational changes, whereas mutants F43L, G47R, and P48S retained the binding of most of the anti-CD4 antibodies tested. The mutants d42–49, Q40P, F43L, and G47R lost both gp120 and class II MHC binding as well as the ability to enhance T-cell activation. In contrast, the mutation P48S affected neither gp120 binding, nor class II MHC binding, nor T-cell activation. We conclude that within this region the binding sites for gp120 and for class II MHC molecules overlap and that amino acids Phe^{43} and Gly^{47} comprise an intimate part of both binding sites. These observations are consistent with a three-dimensional model of the V1 domain of CD4 that was developed in order to understand the structural basis for binding to CD4.**

The CD4 molecule is a surface glycoprotein, expressed in T cells, that associates with the class II major histocompatibility complex (MHC) molecules on the surface of antigen-presenting cells (1–3). When the T-cell receptor (TCR) recognizes antigen in association with class II MHC molecules, the CD4 molecule binds the class II MHC molecule, enhancing a sometimes weak immune interaction (1, 2). The CD4 glycoprotein is also the receptor for the human immunodeficiency virus (HIV), binding the viral envelope glycoprotein gp120 (4).

The CD4 molecule is a single-chain 55-kDa protein with a 372-amino acid extracellular domain consisting of four immunoglobulin-like VJ (variable–joining) or CJ (constant–joining) regions, a 23-amino acid transmembrane domain, and a 38-amino acid cytoplasmic domain (5). The VJ-like (V1) domain of CD4 is 35% homologous to immunoglobulin κ light-chain variable regions (6). Soluble forms of the V1 domain appear to block HIV infectivity and syncytium formation *in vitro* (7–9). Furthermore, epitope-loss mutants of CD4 identified amino acids in the area of residues 42–49 as important for syncytium formation (10). Homolog scanning mutational analysis identified a region between residues 42 and 55 that affects gp120 binding (7, 11). In addition, a much broader region was found to be involved in class II MHC binding compared to that seen affecting gp120 (12, 13).

The publication costs of this article were defrayed in part by page charge payment. This article must therefore be hereby marked "*advertisement*" in accordance with 18 U.S.C. §1734 solely to indicate this fact.

Here we report a series of epitope-loss mutants of CD4, involving amino acids 42–49. These mutants were expressed in a T-cell hybridoma that is dependent on CD4 for efficient immune function. Binding of a panel of anti-CD4 antibodies was carried out to determine the effect on the conformation of the molecule. The effect of mutations on the binding of gp120 and class II MHC-bearing B cells, and on the ability of the mutant CD4 molecule to enhance the T-cell response to antigen, was assessed.

These results were found to be consistent with a three-dimensional model of the N-terminal domain we derived from immunoglobulin crystal structures.

MATERIALS AND METHODS

Mutant Expression. The epitope-loss mutants of CD4 (10) were cloned into the pMNC expression vector previously described. The mutants in this vector were transfected into the retroviral packaging line DAMP, and these DAMP cells were used as the source of retrovirus to infect the T-cell hybridoma By155.16 (1). Infected By155.16 cell lines were screened for CD4 and TCR expression levels by staining with OKT4 (14) or F23.1 (15) monoclonal antibody (mAb), respectively, and analyzed by flow cytometry (1).

Cells expressing CD4 and TCR were stimulated with plate-bound anti-murine CD3 mAb 145-2C11 and assayed for interleukin 2 (IL-2) production. Culture supernatants were assayed for IL-2 by their ability to support the proliferation of the IL-2-dependent line CTLL20 (16) as assessed by the 3-(4,5-dimethylthiazol-2-yl)-2,5-diphenyltetrazolium bromide (Sigma) assay (17, 18). Data are presented as units/ml relative to the OD of CTLL20 from a recombinant human IL-2 (Amgen Biologicals) supernatant. The half-maximal cleavage from the recombinant IL-2 titration was defined as 100 units of IL-2 per ml. Cell lines that produced levels of IL-2 comparable to 16CD413.13, a T-cell hybridoma expressing wild-type CD4, were used for subsequent analysis.

Stimulation Assay. The production of the murine T-cell hybridoma has been described (1). Briefly, C57BL/6 spleen cells from mice immunized with the human Epstein–Barr virus-transformed lymphoblastoid line JY (HLA-A2,2; -B7,7; -DR4,6) were fused with the hypoxanthine/aminopterin/thymidine (HAT)-sensitive thymoma BW5147. The T-cell hybridoma By155.16, which produces IL-2 in response to the class II HLA-DR antigens on JY and Daudi cells, was isolated. The hybridoma was infected with a

Abbreviations: CSE, conserved structural element; HIV, human immunodeficiency virus; IL-2, interleukin 2; mAb, monoclonal antibody; MHC, major histocompatibility complex; TCR, T-cell receptor.

†Present address: BASF Bioresearch Corp., Cambridge, MA 02139.

retroviral expression vector containing the wild-type or mutated CD4 cDNA. The T-cell hybridomas expressing CD4 (5×10^4 cells) were cocultured with Daudi (2×10^5) and after 24 hr the culture supernatants were assayed for the presence of IL-2 with the CTLL20 bioassay.

Immunofluorescent Staining. The cells were stained with a panel of mAbs: anti-Leu-3a (5 μg/ml), OKT4 (1:10 dilution of ascites), OKT4A (5 μg/ml), OKT4B (5 μg/ml), OKT4C (5 μg/ml), OKT4D (5 μg/ml), OKT4E (5 μg/ml), OKT4F (5 μg/ml), T4 (0.25 μg/ml), MT151 (5 μg/ml), and F23.1 (culture supernatant, neat) in 50 μl of phosphate-buffered saline with 5% fetal bovine serum and 0.02% sodium azide for 30 min on ice. Cells were washed, incubated with fluorescein-conjugated goat anti-mouse immunoglobulin, washed, fixed with 0.7% paraformaldehyde, and analyzed by flow cytometry (1).

Conjugate Assay. The measurements of conjugates were performed as described (19). Briefly, hybridoma cells (2×10^6) in 2.0 ml of complete RPMI 1640 medium were labeled with 12 μl of fluorescein diacetate (10 μg/ml) for 10 min at 37°C. These cells were washed three times with complete RPMI and adjusted to 10^6 per ml. Daudi cells were adjusted to 4×10^6 per ml in complete RPMI and 15 μl was added to 15 μl of hybridoma cells. The cells were spun at 250 rpm for 2 min and then incubated for 20 min at 37°C. Conjugates were counted using a fluorescent microscope, with a conjugate being defined as a hybridoma bound to one or more Daudi cells. Results are expressed as the (number of conjugates/total number of hybridoma cells) × 100.

CD4 Modeling. Region A (Lys^{29}–Leu^{44}) of CD4 was modeled as follows. First, by using MACROMODEL 2.5 (20), an oligopeptide was created using the GROW command to place Lys^{29}–Ile^{36} in a β-sheet conformation, Leu^{37} and Gly^{38} in a type II β-turn conformation, and Asn^{39}–Leu^{44} in a β-sheet conformation. This structure was then manipulated to yield the desired mismatched antiparallel β-sheet, and the energy was minimized using the AMBER force field (21, 22) and the BDNR (23) method until the first-derivative root-mean-square gradient was <0.01 kJ/Å·mol. The local conformational space was then searched for lower-energy structures by using molecular dynamics methods of Still (24). The initial minimized structure was heated to 300 K for 5 psec with a time step of 0.5 fsec, and all structures with greater than a 0.5 Å root-mean-square deviation from the initial geometry were saved. The resulting 18 structures were then minimized as before until their first-derivative root-mean-square gradients were <0.05 kJ/Å·mol.

The lowest energy structure was then substituted for the native loop in the REI structure [a Bence-Jones dimer (25)] and the geometry of the area of attachment was optimized using the ANNEAL command in SYBYL 5.1 (Tripos Associates, Saint Louis), which minimized the local area (atoms within a 1-Å radius of the attachment sites) by using the AMBER force field and SYBYL default parameters.

RESULTS

Expression of Mutant CD4 in a Murine T-Cell Hybridoma. CD4 mutants generated by Peterson and Seed (10) were expressed in our T-cell hybridoma. Five mutants in the V1 domain of CD4 were chosen for study. These mutants encompassed a region (amino acids 42–49) suggested to be important to both gp120 and class II MHC binding (11, 13). One of the mutants (d42–49) had a complete deletion of this region from a Ser^{42} to a Ser^{49}. The other mutations (Q40P, F43L, G47R, and P48S) were all single amino acid substitutions and are described by single-letter code for the amino acids involved and the position of the mutation. The retroviral expression vector pMNC was used to express the mutant CD4 cDNA clones in the T-cell hybridoma By155.16 as described (1). After infection of By155.16 with a mutant CD4 cDNA, the level of CD4 expression was assessed by indirect staining using OKT4, an antibody that binds to the membrane-proximal (V4) domain (4) (data not shown). Those cell lines expressing mutant CD4 and also demonstrating TCR expression, as shown by indirect immunofluorescence with the mAb F23.1 (data not shown), were selected for further study. Cell lines were also assessed for their ability to produce IL-2 when stimulated through the CD3 complex by a plate-bound anti-CD3 mAb, 145-2C11 (data not shown). Cell lines producing similar amounts of IL-2 in response to plate-bound 145-2C11 were used to assess the effect mutations in CD4 had on the function of CD4.

Mutations Have Variable Effects on the Overall Conformation of CD4. The effect of a mutation on the conformation of CD4 was examined by assessing the binding of a panel of 10 different anti-CD4 mAbs that bind to the V1 or V1+V2 domain (Table 1). All of the mutant CD4 cell lines expressed the OKT4 epitope but different patterns of expression of the other epitopes. Two of the mutations, d42–49 and Q40P, had dramatic effects on the conformation of the CD4 molecule. The deletion mutant d42–49 completely lost all of the mAb epitopes in the V1 and V2 domains with the exception of that recognized by OKT4D, which bound only minimally to this mutant. The Q40P mutant lost all of the mAb epitopes tested except that of OKT4E, which this mutant bound at levels comparable to that of wild-type CD4. The other three mutants, F43L, G47R, and P48S, had a limited effect on the conformation of CD4. All of these mutants bound most of the antibodies tested at levels similar to that of the wild-type CD4. Peterson and Seed (10) selected the mutants tested here for their reduced ability to bind a particular mAb. The F43L mutant has lost the ability to bind the anti-CD4 mAb, 66.1 (data not shown). The mutation G47R has greatly reduced the binding of OKT4D, and P48S has reduced binding of the mAb T4.

Binding of HIV gp120 to CD4 Mutants. The mutants expressed in our T-cell hybridoma were examined for their ability to bind monomeric gp120 in an indirect immunofluorescence assay quantitated by flow cytometry (Fig. 1). The $CD4^-$ hybridoma By155.16 did not bind gp120, whereas the hybridoma expressing wild-type CD4 showed significant binding of gp120. Of the mutants, only P48S showed binding of gp120 comparable to that of wild-type CD4. The deletion d42–49 and the mutations Q40P, F43L, and G47R all resulted in the inability to bind monomeric gp120.

Effect of CD4 Mutants on T-Cell Hybridoma Function. The function of the CD4 mutants was assessed by the ability of the mutant $CD4^+$ T-cell hybridomas to respond to antigen in

Table 1. Anti-CD4 antibody binding to CD4 mutants

mAb	WT	d42–49	Q40P	F43L	G47R	P48S
OKT4	+++	+++	+++	+++	+++	+++
Anti-Leu-3a	+++	−	−	+++	+++	+++
OKT4A	+++	−	−	+++	+++	+++
OKT4B	+++	−	−	+++	+++	+++
OKT4C	+++	−	−	+++	+++	+++
OKT4D	+++	+	−	+++	+	+++
OKT4E	+++	−	+++	+++	+++	+++
OKT4F	+++	−	−	+++	+++	+++
MT151	+++	−	−	+++	+++	+++
T4	+++	−	−	+++	+++	++

Murine T-cell hybridomas expressing human wild-type (WT) or mutant CD4 were subjected to indirect immunofluorescent staining with a panel of anti-CD4 antibodies at concentrations saturating for wild-type CD4. Analysis was carried out with a FACScan flow cytometer (Beckman). Results are presented as binding equal to that of OKT4 (+++) and as no detectable binding (−) (−, 0–10%; +, 10–30%; ++, 30–80%; +++, 80–100%).

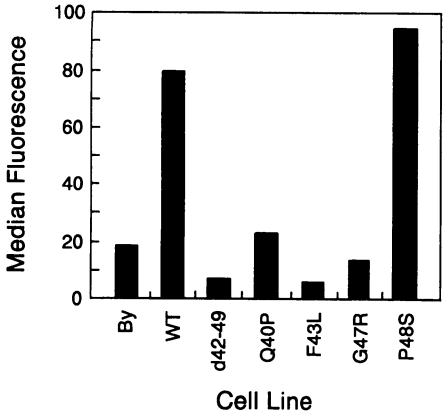

FIG. 1. Binding of gp120 to CD4 mutants. Murine T hybridoma cells expressing either wild-type (WT) human CD4 or mutants of CD4 were incubated with gp120 (20 μg/ml) and binding was detected by indirect immunofluorescent staining using an anti-gp120 mAb followed by fluoresceinated goat anti-mouse antibody. $CD4^-$ cells [T-cell hybridoma By155.16 (By)] were treated similarly. Controls were not incubated with gp120. Analysis was by flow cytometry (FACScan, Beckman). Results are expressed as specific median fluorescence intensity (experimental median fluorescence − control median fluorescence).

comparison to By155.16, the $CD4^-$ hybridoma, or the wild-type $CD4^+$ hybridoma (Fig. 2 *Upper*). Mutants d42–49, Q40P, F43L, and G47R all failed to demonstrate any increased response to antigen. The P48S mutant produced as much IL-2 when stimulated with antigen as the wild-type $CD4^+$ hybridoma. The P48S response was comparable to the response of wild-type CD4 over a range of 2 orders of magnitude of stimulator cells (data not shown). The enhanced IL-2 production of the P48S hybridoma was completely inhibited by the addition to the culture of the anti-CD4 mAb (anti-Leu-3a; data not shown). Thus only P48S retained CD4 function, whereas the d42–49, Q40P, F43L, and G47R all completely lost the ability to enhance the antigen-specific response of the T-cell hybridoma.

Binding of Daudi Cells to CD4 Mutants. The enhancement of the T-cell response by CD4 is initiated by the binding of the class II MHC molecule. The effect mutations of CD4 had on the binding of class II molecules was assessed by a conjugate assay (Fig. 2 *Lower*). The hybridomas were labeled with fluorescein diacetate and then incubated with unlabeled Daudi cells. The number of conjugates formed between the hybridoma and Daudi cells were counted under a fluorescence microscope using both fluorescent and polarized light. The results correlate directly with the stimulation assay. The parental $CD4^-$ hybridoma, By155.16, formed <10% conjugates with Daudi cells, while the hybridoma expressing wild-type CD4 demonstrated ≈20% conjugates with Daudi. The mutants d42–49, Q40P, F43L, and G47R all bound Daudi cells at the same level as the $CD4^-$ hybridoma By155.16. Only the P48S mutant was able to bind to Daudi cells at a level similar to that of the wild-type CD4. The binding by the wild-type CD4 (21.5%) and the P48S (20.8%) mutant to Daudi cells was reduced (4.9% and 6.0%, respectively), by the addition of OKT4F, levels similar to that of the $CD4^-$ hybridoma. These data support the involvement of the wild-type CD4 and the P48S mutant in the binding to Daudi cells.

Construction of a CD4 Model. A better understanding of the functional results obtained with the CD4 mutants was sought by using a hypothetical three-dimensional model of the V1 domain based on immunoglobulin crystal structures. Although the data presented here lend support to the gross geometry of the model, the precise positioning of specific side

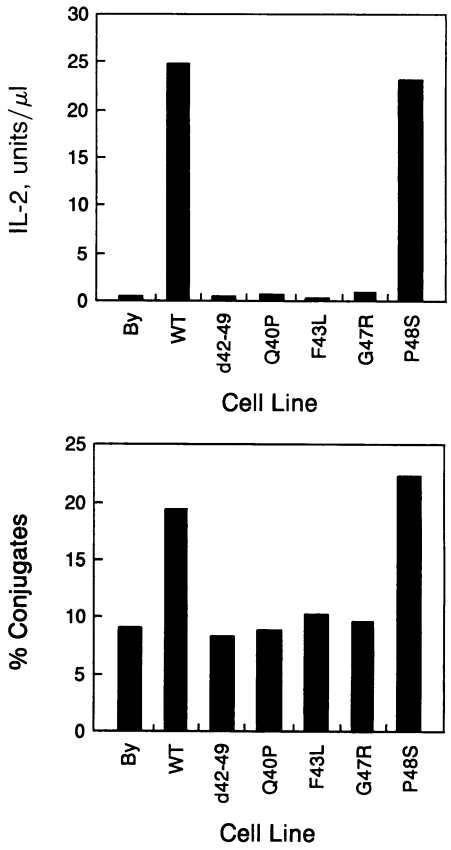

FIG. 2. Stimulation and binding of CD4 mutants by MHC class II^+ Daudi cells. (*Upper*) Stimulation of CD4 mutants. The $CD4^-$ cell line By155.16, $CD4^+$ cell line 16CD413.13 (wild-type, WT), and mutant $CD4^+$ cell lines were stimulated with Daudi cells and IL-2 production was assessed. (*Lower*) Daudi cell binding. The $CD4^-$ cell line By155.16, $CD4^+$ cell line 16CD413.13 (WT), and mutant $CD4^+$ cell lines were fluorescently labeled and cocultured with Daudi cells at a ratio of 1:4. Conjugates were assessed with a fluorescence microscope using both fluorescent and polarized light. Conjugates were assessed as percent of hybridoma cells conjugated to one or more Daudi cells. Results are given as means of three independent experiments (SD <5% of means).

chains and some secondary structural elements such as the C–C′ loop is uncertain.

The first step in model building was to properly align the immunoglobulin and CD4 amino acid sequences (Fig. 3). The human, rat, mouse, and sheep CD4 sequences were first aligned with each other to form a CD4 set, which was then aligned with a set of similarly prealigned immunoglobulin variable regions. Guided by the indicated alignment, the REI structure [a Bence-Jones dimer (25)] was used as a framework for the construction of CD4.

In the REI C–C′ loop there is a 1-residue mismatch between strands, so the longer C′ strand contains a β-bulge and twists slightly around the other strand. In CD4 there is a 2-residue mismatch making the C strand longer, so a CD4 substructure with the opposite twist-handedness of the REI β-sheet in this region was generated *de novo* as described in *Materials and Methods*.

The substitution of nonhomologous REI residues for CD4 residues was made using the CHANGE command in SYBYL. Side-chain steric interactions were corrected using the SCAN command in SYBYL. For the substitution of REI Thr^{72} by CD4 Pro^{59}, the surrounding region was "ANNEALed" to improve the peptide backbone geometry. Finally, the entire structure was minimized using the AMBER force field (Fig. 4 *Upper*). Least-squares superimposition of the resultant and

```
                1                                                    38
   Ratcd4       KTV VLGK.EGGSA ELPCESTSRR SASFAWKSSD QKTIL....G
   Muscd4       KTL VLGK.EGESA ELPCESSQKK ITVFTWKFSD QRKIL....G
 Sheepcd4       KAV VLGK.AGGTA ELPCQASQKN .IVFTWK<---   unknown
     1rei  DIQMTQSPSS LSAS.VGDRV TITCQASQDI IKYLNW.YQ. Q.T.P....G
     1fbj  EIVLTQSPAI TAAS.LGQKV TITCSASSS. VSSLHW.YQ. Q.K.S....G
      CSEs   +  +     @ +   &  +  + + +        + + *+  *        &
   Humcd4       KKV VLGK.KGDTV ELTCTASQKK SIQFHWKNSN QIKIL....G
  Bates-A        KK VVLGKKGDTV ELTCTASQKK SIQFHW.KN. S.N.......
  Bates-B        KK VVLGKKGDTV ELTCTASQKK SIQFHW.KN. S.N.QIKILG
                                                  <-----Region A-

          39                                                     76
   Ratcd4  YKNK.LLIKG .SLEL..... ..YSRFDSRK N..AWERG.S FPLIINKLRM
   Muscd4  QHGKGVLIRG GSPSQ..... ..FDRFDSKK G..AWEKG.S FPLIINKLKM
 Sheepcd4                    unknown   --->W..LWDQG.S K<-unknown
     1rei  KAPKLLIYEA ..SNLQAGV. ..PSRFSGSG S..G...T.D YTFTISSLQP
     1fbj  TSPKPWIYEI ..SKLASGV. ..PARFSGSG S..G...T.S YSLTINTMEA
      CSEs    * *++                 && +             +   +  &
   Humcd4  NQGS.FLTKG .PSKL..... ..NDRADSRR S..LWDQG.N FPLIIKNLKI
  Bates-A  QI.KILGNQG ..SFLTKGPS KLNDRADSRR SLWD...QGN FPLIIKNLKI
  Bates-B  NQGSFLTKGP ..SKLNDRAD ...SRRSLWD Q..G...N.. FPLIIKNLKI
           ---->       <-Region B->            <C>

          77                          103
   Ratcd4  EDSQTYVCEL ENKKEEVELW VFRVTFNPGT RLLQGQSLTL ILDSNPKVSD
   Muscd4  EDSQTYICEL ENRKEEVELW VFKVTFSPGT SLLQGQSLTL TLDSNSKVSN
     1rei  EDIATYYCQQ YQSLPYTFGQ GTKLQIT
     1fbj  EDAAIYYCQQ WTYPLITFGA GTKLELKRAD AAPTVSIFPP SSEQLTSGGA
      CSEs   & + +*+ *          *+  ++ +@+@
   Humcd4  EDSDTYICEV EDQKEEVQLL VFGLTANSDT HLLQGQSLTL TLESPPGSS.
  Bates-A  EDSDTYICEV EDQKEEVQLL .VFGLTANSD THLLQGQSLT LTLESPPGSS
  Bates-B  EDSDTYICEV EDQKEEVQLL .VFGLTANSD THLLQGQSLT LTLESPPGSS
```

FIG. 3. CD4 alignments. Ratcd4, Muscd4, Sheepcd4, and Humcd4, rat (26), mouse (27), sheep (28), and human (5) CD4 sequences; 1rei and 1fby, Brookhaven identifiers for Bence-Jones protein REI (25) and galactan-binding immunoglobulin Fab J539 (29), respectively; Bates-A and Bates-B, alignments of human CD4 proposed by Bates *et al.* (30); CSEs, conserved structural elements in the immunoglobulin family (31): +, intradomain; *, interdomain; &, turn; @, variable–constant chains interface.

REI in regions bordering the insertion/deletion areas (i.e., Lys^{2}–Trp^{28} and Gly^{65}–Asn^{103} of CD4 with Ser^{9}–Trp^{35} and Thr^{69}–Thr^{107} of REI) yielded a root-mean-square deviation of 0.73 Å^2 for all atoms, 0.63 Å^2 for the backbone atoms, and 0.49 Å^2 for the backbone α-carbons (Fig. 4 *Lower*).

DISCUSSION

We have expressed a series of CD4 V1 domain mutants in a T-cell hybridoma that is specific for human class II MHC antigen but is dependent on CD4 for efficient function. Based on the loss of binding by a panel of anti-CD4 mAbs, the d42–49 and the Q40P mutation appeared to have a marked effect on the conformation of the V1 domain. The deletion mutant d42–49 and the substitution mutants Q40P, F43L, and G47R all lost binding of both gp120 and class II MHC molecules, while the P48S mutation did not affect either gp120 binding or class II MHC molecule binding to CD4. There was variable expression of CD4 for the various mutants; however, expression did not affect function, for P48S was one of the lowest expressing mutants. Mutations affecting gp120 binding also affected class II MHC binding, suggesting that these two binding sites overlap in this region.

In order to interpret these data a CD4 model was constructed. Aligning a pre-aligned set of CD4 sequences with a set of immunoglobulin sequences helped resolve uncertainties in the alignment, since different CD4 proteins have retained different residues homologous to the rest of the immunoglobulin superfamily. For example, another alignment of CD4 and REI pairs Arg^{61} of REI with Arg^{58} of CD4 (30), while the rat and mouse CD4 sequences suggest that Arg^{61} of REI ought to be paired with Arg^{54} of CD4 (Fig. 4). Our alignment also considered residues in immunoglobulin CSEs (32), residue chemical properties, and the ability of immunoglobulin regions to accommodate insertions or deletions, as determined by examining immunoglobulin structures.

Most immunoglobulin CSEs are retained in our alignment, except for interdomain CSEs, which is reasonable assuming

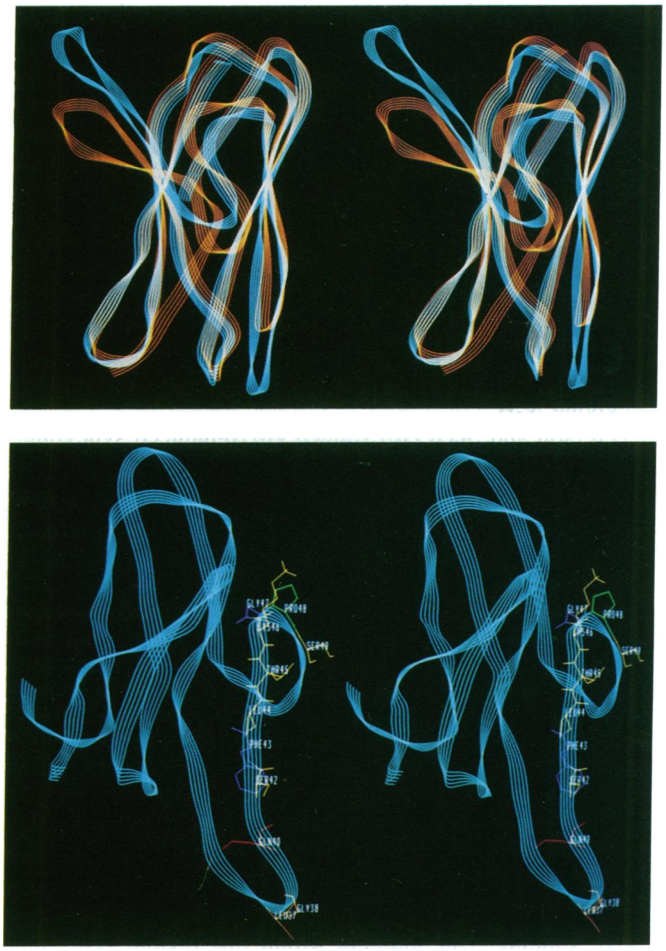

FIG. 4. (*Upper*) Comparison of the CD4 model (cyan) and the REI crystal structure (red-orange). A least-squares superimposition of the structures was made, and the result is shown as ribbon traces through the backbone atoms. (*Lower*) Close-up of the CD4 model showing the C–C′ loop. The model is shown in cyan, and some residues in the C–C′–C″ (C, C′, and C″ are β-strands) region are colored yellow. The model coordinates are available upon request.

that CD4 is monomeric. Most of the hydrophobic side chains interacting between the light and heavy chains in 1IG2 [Brookhaven identifier for IgG KOL (33)] are also mostly absent from CD4. Additionally, a salt bridge and a cystine disulfide "pin" region are highly conserved immunoglobulin structures that are retained in CD4 by our alignment. The salt bridge consists of an arginine and an aspartate (Arg^{61} and Asp^{52} in REI), and the adjacent glutamate and the region near Cys^{84} make it clear that, of the two aspartates in the regions, it is Asp^{78} of CD4 that is homologous to Asp^{82} of REI, while the arginine alignment was previously discussed.

Small amino acid sequence changes can disrupt the tertiary structures of proteins, seriously compromising ligand binding. Two of our CD4 mutations (d42–49 and Q40P) resulted in a loss of binding of most of our panel of mAbs, suggesting major CD4 conformational changes consistent with our model. The deletion d42–49 removes a β-strand connecting two distant parts of the protein, whereas the Q40P mutation can exert a similar effect by producing a kink in the middle of a previously β-sheet region, by virtue of the high β-turn-forming propensity of the Pro-Gly sequence thus introduced. However, our data suggest that such extensive conformational changes cannot be used to explain the loss of ligand binding resulting from the mutations F43L and G47R, since these two mutant CD4 molecules bound most of the mAbs to the same extent as did wild-type CD4.

In our model both Phe^{43} and Gly^{47} are on the highly accessible exposed (C′) side of the C–C′ loop. Whereas the G47R mutation results in a restriction of possible ψ and ϕ angles, the F43L mutation simply entails an exchange of one alkyl side chain for another and should thus have little effect on the backbone conformation. The absence of binding to gp120 in this mutant, therefore, suggests that this side chain may be directly involved in the molecular recognition of gp120. The P48S mutation did not disrupt gp120 or class II MHC binding, which might have been expected, since this Pro^{48} is in a loop region in our model and does not seem to play any explicit structural role, such as β-turn nucleation. Nevertheless, a Pro → Ser mutation would be expected to have a minimal effect since serine often acts like proline in β-turns (34), probably through hydrogen bonding of O^{γ} by the backbone N-H.

Peterson and Seed (10) studied gp120-induced syncytium formation with these mutants expressed in HeLa cells. Their results showed that Q40P permitted marginal syncytia whereas F43L was completely competent in syncytium formation. Our results failed to detect gp120 binding to either of these mutants. The discrepancy may be explained in that syncytium formation involves a multimeric interaction resulting in a detectable avidity, whereas the monomeric gp120 binding assay might be unable to measure binding due to low affinity.

Others have studied the binding of cells bearing class II MHC to cells expressing mutants of CD4. Clayton *et al.* (12) observed class II MHC binding to COS cells expressing the mutant Q40H. Likewise, Lamarre *et al.* (13) found that class II-expressing cells rosette with, and are capable of stimulating IL-2 production in, a hybridoma expressing mutations involving amino acids 39 and 40 (13). While the Q40H was included in the mutations 39–43, neither of the changes in these systems seemed to have a negative effect on class II MHC binding. Our mutants within this region, Q40P and F43L, do not bind gp120 or class II MHC-bearing cells. The difference in the results for the mutation at residue 40 may be explained by the disruptive effects brought on by the substitution of a proline in our mutant. The F43L mutation, a relatively conservative change of a nonpolar residue for another nonpolar residue, caused a loss of binding of class II MHC molecules as well as gp120, whereas Lamarre *et al.* (13) found that four different mutations together in the region 39–43 retained class II MHC binding but lost gp120 binding (13). With multiple mutations in this region, it is difficult to determine the importance of individual residues within the region based on this type of analysis. In the case of F43L, this seems to be an important residue in the interaction of gp120 and class II MHC with CD4 because of the dramatic effects it has on the binding of these molecules in the context of the less drastic changes in the conformation of CD4. Our results with the mutant P48S agree with the findings of Lamarre *et al.* for this region in that both gp120 and class II MHC bound to this mutant. Lamarre *et al.* changed four residues between amino acids 48 and 52 and retained binding when this mutant CD4 was expressed in a T-cell hybridoma. Clayton *et al.* (12), on the other hand, expressed three of the same four mutations in COS cells (one of these three being residue 48) and lost both gp120 and class II MHC binding. The differences in the results in these two systems may be due to the cell types in which the CD4 was expressed, subtly affecting the final conformation of the molecule.

Finally, we interpret these results to suggest that the binding sites for gp120 and class II MHC on CD4 overlap between amino acids 42 and 49. Further, given the conservative substitution, Phe^{43} appears to be particularly important to both of these interactions. We suggest that the local geometry centering about Phe^{43} in the CD4 V1 model presented herein should serve as a basis for the design of small-molecule antagonists of CD4–gp120 binding interactions (35).

The mAbs OKT4A through OKT4F were generously provided by Dr. P. Rao of Ortho Monoclonals, Raritan, NJ. M.R.B. is the recipient of a National Research Service Award postdoctoral fellowship. K.D.M. is the recipient of a National Science Foundation graduate fellowship. This work was supported by grants from the National Institutes of Health to S.J.B. (AI17258) and to S.L.S. (GM30738-09).

1. Sleckman, B. P., Peterson, A., Jones, W. K., Foran, J. A., Greenstein, J. L., Seed, B. & Burakoff, S. J. (1987) *Nature (London)* **328,** 351–353.
2. Gay, D., Maddon, P., Sekaly, R., Talle, M. A., Godfrey, M., Long, E., Goldstein, G., Chess, L., Axel, R., Kappler, J. & Marrack, P. (1987) *Nature (London)* **328,** 626–629.
3. Doyle, C. & Strominger, J. L. (1987) *Nature (London)* **330,** 256–259.
4. Sattentau, Q. J. & Weiss, R. A. (1988) *Cell* **52,** 631–633.
5. Maddon, P. J., Littman, D. R., Godfrey, M., Maddon, D. E., Chess, L. & Axel, R. (1985) *Cell* **42,** 93–104.
6. Williams, A. F. & Barclay, A. N. (1988) *Annu. Rev. Immunol.* **6,** 381–405.
7. Arthos, J., Deen, K. C., Chaikin, M. A., Fornwald, J. A., Sathe, G., Sattentau, Q. J., Clapham, P. R., Weiss, R. A., McDougal, J. S., Pietropaolo, C., Axel, R., Truneh, A., Maddon, P. J. & Sweet, R. W. (1989) *Cell* **57,** 469–481.
8. Traunecker, A., Lake, W. & Karjalainen, K. (1988) *Nature (London)* **331,** 84–86.
9. Berger, E. A., Fuerst, T. R. & Moss, B. (1988) *Proc. Natl. Acad. Sci. USA* **85,** 2357–2361.
10. Peterson, A. & Seed, B. (1988) *Cell* **54,** 65–72.
11. Clayton, L. K., Hussey, R. E., Steinbrich, R., Ramachandran, H., Husain, Y. & Reinherz, E. L. (1988) *Nature (London)* **335,** 363–366.
12. Clayton, L. K., Sieh, M., Pious, D. A. & Reinherz, E. L. (1989) *Nature (London)* **339,** 548–551.
13. Lamarre, D., Ashkenazi, A., Fleury, S., Smith, D. H., Sekaly, R. P. & Capon, D. J. (1989) *Science* **245,** 743–746.
14. Reinherz, E. L., Kung, P., Goldstein, G. & Schlossman, S. (1979) *Proc. Natl. Acad. Sci. USA* **76,** 4061–4065.
15. Staetz, U., Rammensee, H. G., Benedetto, J. S. & Bevan, M. J. (1985) *J. Immunol.* **134,** 3994–4000.
16. Gillis, S., Ferm, M. M., Ou, W. & Smith, K. A. (1978) *J. Immunol.* **120,** 2027–2031.
17. Gerlier, D. & Thomasset, N. (1986) *J. Immunol. Methods* **94,** 57–63.
18. Mosmann, T. (1983) *J. Immunol. Methods* **65,** 55–62.
19. Takai, Y., Reed, M. L., Burakoff, S. J. & Herrmann, S. H. (1987) *Proc. Natl. Acad. Sci. USA* **84,** 6864–6868.
20. Mohamadi, F., Richards, N. G. J., Guida, W. C., Liskamp, R., Lipton, M., Caufield, C., Chang, G., Hendrickson, T. & Still, W. C. (1990) *J. Comput. Chem.* **11,** 440–467.
21. Weiner, S. J., Kollman, P. A., Case, D. A., Singh, U. C., Chio, C., Algona, G., Profeta, S., Jr., & Weiner, P. (1984) *J. Am. Chem. Soc.* **106,** 765–784.
22. Weiner, S. J., Kollman, P. A., Nguyen, D. T. & Case, D. A. (1986) *J. Comput. Chem.* **7,** 230–252.
23. Burkert, U. & Allinger, N. L. (1982) *Molecular Mechanics*, ACS Monograph 177 (Am. Chem. Soc., Washington, DC).
24. Still, W. C. (1987) in *Stereochemistry of Organic and Bioorganic Transformations*, eds. Bartmann, W. & Sharpless, K. B. (VCH, New York), pp. 235–246.
25. Epp, O., Lattman, E. E., Schiffer, M., Huber, R. & Palm, W. (1975) *Biochemistry* **14,** 4943–4952.
26. Clark, S. J., Jefferies, W. A., Barclay, A. N., Gagnon, J. & Williams, A. F. (1987) *Proc. Natl. Acad. Sci. USA* **84,** 1649–1653.
27. Maddon, P. J., Moleneaux, S. M., Maddon, D. E., Zimmerman, K. A., Godfrey, M., Alt, F. W., Chess, L. & Axel, R. (1987) *Proc. Natl. Acad. Sci. USA* **84,** 9155–9159.
28. Classon, B. J., Tsagaratos, J., McKenzie, I. F. C. & Walker, I. D. (1986) *Proc. Natl. Acad. Sci. USA* **83,** 4499–4503.
29. Suh, S. W., Bhat, T. N., Navia, M. A., Cohen, D. N., Rudikoff, S. & Davies, D. R. (1986) *Proteins Struct. Funct.* **1,** 74–80.
30. Bates, P. A., McGregor, M. J., Islam, S. A., Sattentau, Q. J. & Sternberg, M. J. E. (1989) *Protein Eng.* **3,** 13–21.
31. Chothia, C., Boswell, D. R. & Lesk, A. M. (1988) *EMBO J.* **7,** 3745–3749.
32. Chou, P. Y. & Fasman, G. D. (1977) *J. Mol. Biol.* **115,** 135–141.
33. Marquart, M., Deisenhofer, R., Huber, R. & Palm, W. (1980) *J. Mol. Biol.* **141,** 369–391.
34. Aubry, A. & Marraud, M. (1983) *Biopolymers* **22,** 341–345.
35. Finberg, R., Diamond, D. C., Mitchell, D. B., Rosenstein, Y., Soman, G., Norman, T. C., Schreiber, S. L. & Burakoff, S. J. (1990) *Science* **249,** 287–291.